

# NG2-expressing glial precursor cells are a new potential oligodendrogloma cell initiating population in N-ethyl-N-nitrosourea-induced gliomagenesis

Anne Briançon-Marjollet<sup>1</sup>, Laurent Balenci<sup>1</sup>, Manuel Fernandez<sup>2,3</sup>, François Estève<sup>2,3</sup>, Jérôme Honnorat<sup>4</sup>, Régine Farion<sup>2</sup>, Marine Beaumont<sup>2</sup>, Emmanuel Barbier<sup>2</sup>, Chantal Rémy<sup>2</sup>, Jacques Baudier<sup>1\*</sup>

<sup>1</sup> Transduction du signal : signalisation calcium, phosphorylation et inflammation INSERM : U873 , CEA : DSV/IRTSV , Université Joseph Fourier - Grenoble I , CEA 17, rue des martyrs IRTSV - LTS 38054 GRENOBLE CEDEX 9,FR

<sup>2</sup> GIN, Grenoble Institut des Neurosciences INSERM : U836 , CEA , Université Joseph Fourier - Grenoble I , CHU Grenoble , UJF - Site Santé La Tronche BP 170 38042 Grenoble Cedex 9,FR

<sup>3</sup> ESRF, European Synchrotron Radiation Facility ESRF , 6 rue Jules Horowitz BP220 38043 GRENOBLE CEDEX,FR

<sup>4</sup> Neuro-oncologie et neuro-inflammation INSERM : U842 , Université Claude Bernard - Lyon I , Faculté de médecine Laennec rue G. Paradin 69372 Lyon CEDEX 08,FR

\* Correspondence should be addressed to: Jacques Baudier <jbaudier@cea.fr >

## Abstract

Gliomas are the most common primary brain tumor affecting human adults and remain a therapeutic challenge because cells of origin are still unknown. Here, we investigated the cellular origin of low-grade gliomas in a rat model based on transplacental exposure to Nethyl-N-nitrosourea (ENU). Longitudinal magnetic resonance imaging coupled to immunohistological and immunocytochemical analyses were used to further characterize low-grade rat gliomas at different stages of evolution. We showed that early low-grade gliomas have characteristics of oligodendrogloma-like tumors and exclusively contain NG2-expressing slow dividing precursor cells which express early markers of oligodendroglial lineage. These tumor-derived precursors failed to fully differentiate into oligodendrocytes and exhibited multipotential abilities *in vitro*. Moreover, a few glioma NG2+ cells are resistant to radiotherapy and may be responsible for tumor recurrence, frequently observed in humans. Overall, these findings suggest that transformed multipotent NG2 glial precursor cell may be a potential cell of origin in the genesis of rat ENU-induced oligodendrogloma-like tumors. This work may open up new perspectives for understanding biology of human gliomas.

**MESH Keywords** Animals ; Antigens ; analysis ; Brain Neoplasms ; chemically induced ; pathology ; Cell Differentiation ; Cell Line, Tumor ; Ethylnitrosourea ; toxicity ; Neoplastic Stem Cells ; chemistry ; pathology ; Oligodendrogloma ; chemically induced ; pathology ; Proteoglycans ; analysis ; Rats ; Rats, Sprague-Dawley ; ras GTPase-Activating Proteins ; analysis

**Author Keywords** Glial precursor ; Cancer stem cells ; Glioblastoma ; Oligodendrogloma ; NG2 ; neural progenitors

## Introduction

Glioma represent the most common and heterogeneous group of brain tumors emerging in adult human central nervous system. These tumors are traditionally classified according to their histopathology and the cell-type markers they express and lead to a complex classification theme. Nevertheless, glioma can roughly be subdivided into three major subgroups of different grades: (1) astrocytomas: pilocytic (grade I), diffuse (grade II), anaplastic (grade III) and glioblastoma multiform (GBM) (grade IV), (2) oligodendroglomas (grade II and grade III), and (3) mixed oligoastrocytomas. This diversity of glioma correlates with a wide spectrum of mutated or affected cell signaling pathways observed in these neoplasms and also likely due to their different 'cell of origin' [1]. Moreover, in many cases, tumors which share a similar morphology and phenotype may have very different prognoses and responses to therapies. This underlines the need to redefine the criterions of the tumor classification which now will have to deal not only with a molecular and cellular analysis of the tumor bulk, but also on a better understanding of how tumors emerge, evolve over time and what cell types they arise from. Several recent studies have identified a tumorigenic CD133+ subpopulation of cancer cells regarded as tumor stem cells within GBM responsible for the initiation and development of those heterogeneous aggressive brain tumors [2–5]. The presence of cancer stem cells in GBM may also explain the resistance of these tumors to radiotherapy and chemotherapy [6]. In contrast to glioblastomas, oligodendroglomas are more sensitive to radiotherapy and alkylating agent chemotherapy [7,8]. This variable therapeutic responsiveness has raised the hypothesis that oligodendrogloma and glioblastoma may have distinct origins. Transgenic mouse and rat models using controlled ectopic expression of oncogenes in either precursor or maturing astrocytes have been used to model human glioblastoma, astrocytomas, oligodendroglomas, or oligoastrocytomas, depending on the oncogenic stimuli [9–16]. These studies highlight the potential genetic mutations which could be responsible for tumor initiation and development. On the other hand, recent studies have shown that signals from environment can also initiate and mediate tumor growth, as nestin-positive neonatal neural progenitors retrovirally over-expressing PDGF-B generate pure oligodendrogloma, whereas targeting GFAP-expressing glial progenitors gives rise to several types of tumors [17,18]. In order to complement these genetically-induced tumor studies, we here investigated the 'cell of origin' of low-grade glioma in a far known rat model

which spontaneously develops glioma in response to transplacental exposure to the DNA alkylating agent N-ethyl-N-nitrosourea (ENU) [19–23]. ENU-induced tumors have morphological and biological features similar to human glioma [22,24]. ENU-induced tumors mimic the evolution and development of a brain tumor upon a sporadic exposure to carcinogens and neoplasms appear after several months of latency, thus helping with the understanding of early events occurring during gliomagenesis. In this study, we performed longitudinal MRI analysis of ENU-induced glioma over a period of 11 months combined with full characterization of tumor cells at different developmental stages. We identified a new slow dividing NG2 cell population, expressing early markers of oligodendroglial lineage and compromised in their differentiation, in low-grade glioma. *In vitro*, these cells exhibited multipotential abilities. In postnatal/adult brain NG2-expressing cells are strongly associated with fast dividing oligodendrocyte progenitor cells (OPC) [25]. However, heterogeneity of NG2+ cell population has been demonstrated in several occasions. Bouslama-Oueghlani provided evidence that two types of NG2+ cells are present in developing brain, one highly proliferating and able to myelinate axons, and one almost quiescent with a reduced ability to produce myelin [26]. Recent studies have also demonstrated that early postnatal NG2<sup>+</sup> cells are able to form passageable neurospheres and to differentiate into neurons *in vitro* [27] as well as to contribute to postnatal neurogenesis in developing hippocampus and olfactory bulb [28,29]. We also previously found that NG2 marker is expressed in multipotent neurospheres derived from adult SVZ [30]. We propose a potential contribution of these multipotent NG2+ glial precursors in low-grade glioma genesis and recurrence. These findings may help to understand several features observed in human oligodendroglioma and to design new therapies to cure glioma.

## Materials and methods

### Antibodies

The following primary antibodies were used: IQGAP1 (H109, rabbit, 1/500<sup>e</sup>, Santa Cruz Biotechnology), Nestin (clone rat-401, mouse, 1/500<sup>e</sup>, Developmental Studies Hybridoma Bank), NG2 (mouse or rabbit, 1/500<sup>e</sup>, Upstate), Olig2 (rabbit, 1/500<sup>e</sup>, a generous gift from Dr. H. Chneiweiss, INSERM U114, Paris), GFAP (rabbit, 1/500<sup>e</sup>, Dako Cytomation), Sox10 (rabbit, 1/500<sup>e</sup>, a generous gift from Dr. Wegner, Erlangen University, Germany), Nkx2.2 (mouse, 1/100<sup>e</sup>, Developmental Studies Hybridoma Bank), A2B5 (mouse, 1/3, hybridoma production), O4 (mouse, 1/3, hybridoma production),  $\beta$ III-tubuline (clone Tuj-1, rabbit, 1/1000<sup>e</sup>, Eurogentec), Ki67 (mouse, 1/100<sup>e</sup>, AbCys), Collagen IV (goat, 1/1000<sup>e</sup>, Southern Biotech).

Secondary antibodies conjugated to cyanine 3 or cyanine 5 were from Jackson Laboratories (Interchim, France), secondary antibodies conjugated to Alexa Fluor 488 were from Molecular Probes (Invitrogen, France) and biotinylated anti-goat secondary antibody was from Southern Biotech.

### Chemo-induced tumorigenesis

All procedures on animals were approved by the Rhône-Alpes Committee for Animal Experimentation Ethics (CREEA). OFA Sprague-Dawley pregnant rats were obtained from Charles River Laboratories (France). Pregnant rats were injected i.v. via the tail vein with 60mg/kg Ethylnitrosourea (Sigma-Aldrich) at gestational day E19. Five independent ENU injections were done over a period of 3 years, including two to four pregnant animals per experiment.

### Magnetic Resonance Imaging (MRI) of rat brains

MRI images were obtained with a 2.35T magnet using a volume coil for transmission and a surface coil for reception. Anesthetized rats were placed in a cradle and their head was maintained with ear bars and a bite bar. For each animal, 20 contiguous 1 mm-thick slices, were acquired using a T2-weighted spin-echo sequence (TR/TE=2000/80ms, matrix=256\*192 or 128\*128, 2 accumulations, FOV=30\*30 mm<sup>2</sup>).

### Tumor Growth Profile

Tumor volume was calculated using Image J software. Tumor surface (mm<sup>2</sup>) was measured on MRI images according to MRI resolution. Tumor volume was calculated by analyzing the surface of the tumor on successive MRI slices multiplied by slice thickness (1 mm). Two-way Anova statistical analysis was done using Sigma Stat software. Holm-Sidak tests were used for post-hoc multiple comparisons.

### Immunohistochemistry/immunofluorescence

3- to- 12-months old animals were deeply anesthetized with 5% isoflurane and killed by decapitation. Brains were immediately frozen in isopentane at -80°C. 10- $\mu$ m cryosections were cut and postfixed in 4% paraformaldehyde. Sections were colored with hematoxylin and eosin for histological analysis. Alternatively, cryosections were permeabilized in TBS-0.2% Triton and blocked in TBS-5% goat serum. After overnight incubation with primary antibodies, sections were stained with secondary antibodies and counterstained with nuclear marker Hoechst 33258 (1 $\mu$ g/mL) when desired. Images were obtained with a Carl Zeiss Axiovert 200M microscope and with a Leica (TCS SP2) confocal microscope.

Cells or glioma explants were fixed using 4% paraformaldehyde and procedures were the same as brain slices except that incubation times for primary and secondary antibodies were reduced to 1 hour each. Antibodies for cell surface markers, such as A2B5 and O4, were added to culture medium for 1h before cell fixation.

### Oligodendroglioma-derived cell culture

After MRI localization, tumors were excised from freshly dissected rat brains. They were cut in explants and plated onto poly-L-lysine treated glass coverslips, either in proliferation medium with 10ng/mL PDGF and 1 µg/mL bFGF, or in differentiation medium where PDGF and bFGF were replaced by 30ng/mL T3, 5ng/mL CNTF and 5µm Forskolin (as described in Deloulme et al. 2004 and Kondo and Raff 2000 [29]). After 4 to 8 days in culture, cells were fixed in 4% paraformaldehyde. Additionally, a piece of the tumor was frozen in isopentane at -80°C immediately after dissection for immunohistological characterization.

### Rat brain tumor irradiation

Irradiation was performed at the Biomedical beamline of the European Synchrotron Radiation Facility (ESRF). Irradiation was performed with monochromatic synchrotron radiation, emitted from a wiggler multipole magnet. The energy used was 80 keV with a bandwidth of  $\Delta E/E = 10^{-3}$ . The dose delivered to tumors was 15 Gy. The irradiated volume covered a whole hemisphere and it was performed in tomotherapy mode, i.e. rotating the animal in the beam. The animals were anesthetized for irradiation and held vertically in a plastic frame, which kept their heads fixed. Beam dimensions were 1 mm vertical and 10 mm horizontal. Therefore, multistage irradiations were performed to cover the total volume of the brain hemisphere, typically 15 mm in length and 10 mm in diameter.

## Results

### Spatial and temporal emergence and development of rat chemically-induced brain tumors

In this study, we used a well-established experimental model of brain tumors in which rats exposed *in utero* to a single dose of a mutagen, the N-Ethyl-N-NitrosoUrea (ENU) preferentially develop brain tumors [19, 22, 24]. This model has also the advantage of retracing basic events of carcinogenesis following a random exposure to mutagens or chemicals. The latency before appearance of brain tumor enables to address early events occurring in brain tumor genesis. Moreover, the drug is rapidly degraded *in vivo* thus avoiding any side effects causing by inflammatory response [31]. Six months to eleven months after exposure, some exposed animals exhibited severe neurological symptoms and the post-mortem examination revealed the presence of peripheral tumors and/or highly invasive brain tumors. These animals were no further investigated. We focused on exposed rats which showed no pathological evidence of tumor formation, hypothesizing that these might represent earliest stages in tumor occurrence. Longitudinal T2-weighted magnetic resonance imaging (MRI) along with measurements of water diffusion (i.e. ADC = Apparent Diffusion Coefficient) were used to visualize the spatial and temporal emergence of asymptomatic brain tumors. Several brain tumors within a single animal were frequently observed. At 6 months of age, asymptomatic brain tumors showed sizes ranging between 250 µm<sup>3</sup> to 1200 µm<sup>3</sup> and exhibited a homogenous hypersignal on T2-weighted scans (Figure 1a-d). Subsequently, 4 to 5 months later (i.e. at 10–11 months of age) ENU-induced tumors evolved in different ways and allowed us to distinguish 3 tumor subtypes (Type 1 to 3) according to MRI pictures (Figure 1a-d), tumor growth profiles (Figure 1d) and mitotic index (Figure 1e). Type 1 glioma (67%) and Type 2 glioma (17.5%) maintained a homogenous hypersignal on T2-weighted scans (Figure 1a-b). Type 1 gliomas were characterized by a linear growth over time with a doubling volume every 2 to 3 months (Figure 1d). Type 1 glioma mainly located in the corpus callosum (CC) (45%) and in germinative areas (30%) including the anterior subventricular zone and the rostral migratory stream (Supplemental Figure 1a). Type 2-induced glioma followed the same diagram (Figure 1b) but grew almost 3 times faster than types 1 to increase tenfold in size over a period of 5 months (Figure 1d). Type 2 glioma were predominantly located in the corpus callosum (29%) and the cortex (33%) (Supplemental Figure 1b). Type 3 glioma (15%) adopted a 2 phase-pattern, with a slow growth for the first 9 months followed by an exponential growth profile (Figure 1d). MRI analysis of type 3 tumors revealed heterogenous T2-weighted images which ended up with a large hypersignal in tumor cores, surrounded by a hyposignal ring. Type 3 glioma were predominantly observed in the cortex (67%) (Supplemental Figure 1c). In agreement with their growth profiles, 11 months after ENU exposure, Type 3 glioma have the highest mitotic index and Type 2 glioma present 3 times more Ki67+ cells compared to Type 1 neoplasms (Figure 1e).

Histological characterization showed that Type 1 tumors have homogenous cellular density within tumor bulks with a normal vascular network (Figure 1f). Type 2 neoplasms exhibited a mixed population of normal rounded shape and hyperchromatic nuclei with an increased density of blood vessels (Figure 1g). Type 3 glioma exhibit malignant features with a large necrosis along with a very high developed vasculature (Figure 1h).

### Slowly proliferating rat glioma display features of oligodendroglioma

We have previously shown that the most aggressive rat glioma (Type 3) have histologic and immunophenotypic characteristics that resemble human glioblastoma [5]. Both rat and human glioblastoma are characterized by niches of tumorigenic cells which express nestin and IQGAP1 [4, 5]. We here focused on further characterizing lower aggressive rat gliomas (Type 1 and Type 2) in order to identify the potential tumor initiating cells.

In these non malignant rat tumors, the expression of IQGAP1 was restricted to tumor endothelial cells (Figure 2a). The strict association of IQGAP1 immunoreactivity with tumor endothelial cells also characterized low-grade and high grade human oligodendroglioma [5]. In addition, rat tumor cells had a uniform immunophenotype characterized by intense immunoreactivities for the cell surface NG2 proteoglycan and PDGF $\alpha$ -receptor (Figure 2b). NG2 and PDGF $\alpha$ -receptor have been previously shown to be specifically expressed in human oligodendroglioma but not in human glioblastoma [32]. Moreover, NG2+ tumor cells did homogeneously express the nuclear transcription factors Olig2, Nkx2.2 and Sox10 of committed progenitor cells to oligodendroglial lineage [33, 34] (Figure 2c). Previous investigations have demonstrated that the expression of all these markers is associated with human oligodendroglioma [35–37]. None of the tumor cells expressed neither O4, a late marker of oligodendrocyte progenitor cells nor MBP, a marker of mature oligodendrocytes, in any of the rat low-grade induced-glioma (data not shown). In summary, histological and immunological analyses revealed that slowly proliferating rat brain tumors have features that resemble human oligodendroglioma.

### Early low-grade glioma cells are linked to slow-cycling NG2-expressing precursor cells

In the rodent brain, two populations of NG2-expressing cells have been reported with different proliferation, differentiation and migration capacities [25, 26, 28]. NG2- and O4- (late marker of OPC) co-expressing cells account for the biggest pool of postnatal and adult dividing progenitor cells in brain parenchyma and correspond to oligodendrocyte progenitors contributing to oligodendrocytes, the myelinating cells of the central nervous system [25]. Another population of NG2-expressing cells in postnatal brain which possess a low proliferation rate and a limited ability to differentiate into myelinating oligodendrocytes has also been identified [26]. In adult rat brain, NG2-expressing cells represent a major multipotential progenitor population in the germinative subventricular zone (SVZ) and rostral migratory stream (RMS) that gives rise to oligodendrocyte and neurons [27–29]. In the RMS, these cells are concentrated within migrating chains of proliferating  $\beta$ III tubulin+ neuroblasts [28] (Figure 3a). This specific NG2 cell population is characterized by few processes and the nuclear expression of Nkx2.2 [28] and Sox10 (Figure 3b). In contrast to parenchymal NG2+/O4+ OPC and migrating  $\beta$  III tubulin+ neuroblasts, NG2+ precursor cells present within the SVZ and RMS are rarely labelled with the proliferation associated antigen Ki67 (Figure 3c).

To investigate whether low-grade glioma cells could interrelate to slow-cycling NG2+/Nkx2.2+/Sox10+ precursor cells, we focused on early hyperplastic lesions in 3 month-old animals when brain tumors are not yet identifiable by MRI. In order to detect emerging micro-tumors, 20 $\mu$ m brain sections were performed from the olfactory bulb to posterior hippocampus. We then screened brain sections under the microscope to identify putative nascent neoplasms and stained them for NG2 and counterstained with DAPI to find any abnormal cell densities (Figure 4a and Supplemental Figure 2a). In Figure 4 we selected early hyperplastic lesions emerging from the germinative rostral migratory stream (RMS) where low grade oligodendroglioma-like tumors preferentially arose from (Supplemental Figure 1). Tumor cells were homogeneously expressing NG2 (Figure 4a) Sox10 (Figure 4b) and Nkx2.2 (Figure 4c). We next compared the mitotic activity of tumor cells with adjacent migrating neuroblasts. Data show that no more than 5% of NG2-expressing cells did express Ki67 antigen compared to migrating  $\beta$ III tubulin+ neuroblasts, suggesting that low-grade glioma cells are allied to slow-cycling NG2-, Nkx2.2-, Sox10- positive precursor cells (Figure 4d and 4e). These observations were consistent in all early hyperplastic lesions (n =15) found in 3 month-old animals (n=10) irrespective of their location (Supplemental Figure 2).

### Low grade glioma-derived cells are compromised in their differentiation abilities

To further characterize the NG2 cell population present within rat induced low-grade glioma, we next addressed their *in vitro* properties. Several attempts to grow cells from 6–7 months low proliferating glioma as neurospheres or as monolayers were unsuccessful suggesting that cell-cell contacts and signals from environment are crucial for tumor cells to survive and/or proliferate. Therefore, to analyze what properties these tumoral NG2+ cells could have *in vitro*, we cultured tumor explants in media supplemented with PDGF and bFGF to promote multipotent oligodendroglial progenitor proliferation [38]. After 6 days in proliferative conditions, glioma cells continued to express NG2 (Figure 5a–b) and Nkx2.2 (Figure 5a). While cells migrated away from core explants, they changed cell immunophenotype and proliferation characteristics. Migrating cells started to express late OPC markers O4 (Figures 5b) and A2B5 (Supplemental Figure 3). About 30% of the migrating cells acquired O4+ phenotype (Figure 5c). Cells that migrated out of the explant also started dividing faster as 30% of the migrating cells became Ki67+ (Figure 5d and Supplemental Figure 3), compared to less than 5% in original low grade tumors *in vivo* (Figure 1e). This suggests that within the tumor mass, NG2+ cells are maintained in undifferentiated and non proliferative states but can acquire immunological and fast replication characteristics of O4+ late OPC in determined culture conditions. We next addressed whether tumor cells are able to fully differentiate along the oligodendroglial lineage by culturing glioma explants in differentiation medium where PDGF and bFGF are replaced by T3 and forskolin [39]. After 6 days in these specific culture conditions the number of O4+ cells in glioma explant cultures did not significantly increased (Figure 5c) while proliferation slightly

decreased (Figure 5d ). Moreover, no MBP+ cells were detected (data not shown), pointing out that tumoral NG2+ cells can acquire OPC features but fail to fully differentiate into oligodendrocytes. Conversely, in such culture conditions, oligodendrocyte progenitors derived from newborn rat brains sequentially lost NG2 immunoreactivity and started expressing late OPC markers (i.e A2B5 and O4) after 3 days *in vitro* (Supplemental Figure 4a ). By 6 days, some OPC matured into oligodendrocytes as they express the myelin basic protein (MBP) (Supplemental Figure 4b ).

Postnatal NG2+ cells can behave as multipotential precursor cells *in vivo* and *in vitro* and contribute to both gliogenesis and neurogenesis [27–29]–[27,30]. To further investigate whether tumoral NG2+ cells have such multipotential capabilities we cultured glioma explants in serum-containing medium for a week. Results show that glioma NG2+ cells could stably co-express both astrocyte marker GFAP and neuroblast marker  $\beta$ III-tubulin while they were still expressing NG2 and Nkx2.2 markers (Figure 5e–f ). Such aberrant patterns of expression were independent of culture conditions. These observations emphasize the transformed character of these NG2-expressing tumoral precursor cells. Overall, these findings suggest that ENU preferentially targets NG2+ multipotent precursor cells which results in an impairment and/or aberrant differentiation of their progeny rather than an increase in cell proliferation.

### A few tumoral NG2+ cells are resistant to radiations

Currently, therapies for human low-grade gliomas include observation, resection, radiation and chemotherapy. Radiotherapy extends survival but total remissions are rarely observed [40]. In order to determine the response of ENU-induced glioma to radiotherapy, five rats aged of 6 months and carrying low grade glioma were irradiated with a 15 Gy dose in whole brain hemispheres and followed up by MRI for up to 4 months after treatment. From MRI examination, three rats showed an apparent total tumor regression 137 days upon treatment (Figure 6a–b ). Nevertheless, the histological analysis of irradiated tissues revealed the presence of remnant tumor cells which resisted radiations (Figure 6c–d ). Among those surviving cells, 87.6% and 82.6% express Sox10 and Olig2 markers respectively (Figure 6d ). On the other hand, the stem cell markers, nestin and IQGAP1 were still exclusively present in blood vessels. These results suggest that rat low grade glioma are in their majority radiosensitive, as observed for human oligodendroglioma, but some radio-resistant tumor cells persist and could be responsible for tumor recurrence.

## Discussion

Here we used a rat model that develops glioma following *in utero* exposure to the mutagenesis agent N-ethyl-N-nitrosourea to investigate the potential origin of low-grade glioma. Although genetic mutations induced by ENU may be difficult to identify [24], this model provides useful insights about the early events that precede glioma formation and may thus be helpful to identify cells of origin for glioma. Rat low grade gliomas represent the major asymptomatic neoplastic lesions (67%) 6 months after exposure to ENU. Longitudinal imaging analysis revealed that after a latency period of 6 months, some low grade glioma developed into more aggressive tumors (referred as Type 2). Taking into account that both tumor subtypes developed with high frequency in the same brain regions (Supplemental Figure 1 ), it is likely that they might have the same origin. Such modifications in tumor characteristics could be due to changes in tumor environment or to additional mutations.

Within slowly dividing gliomas tumor cells homogeneously expressed the same markers, including cell surface markers NG2 and PDGF $\alpha$ -R and nuclear transcription factors Olig2, Sox10 and Nkx2.2.transcription factors (Figures 2 and Supplemental Figure 2 ), involved in embryonic OPC specification [33,34]. *In situ*, tumor cells did not express O4, a surface marker of late OPC during postnatal development [41] as well as specific of adult OPC which are scattered in the all brain parenchyma [25,42,43]. Several studies have demonstrated the heterogeneity of NG2+ cell population with different proliferation features and differentiation capacities [26,42,44]. Moreover, a population of multipotent NG2+ precursor cells that is able to produce both glial cells and neurons has been identified [27–30,33,38,39,45]. We propose that these multipotent NG2 precursor cells can be a preferential target for ENU-mutagenesis. As we could expect from developmentally- deregulated cells with multipotential competence, *in vitro* tumor cells were characterized by aberrant co-expressions of several cell lineage antigens (Figure 5 ). Longitudinal MRI imaging revealed that rat low grade glioma have a slow and linear growth phase suggesting that the initial transformation process is not primarily associated with a gain in proliferation capacity. We can envision that ENU mutagenesis modified genes that control either the self-limiting extension, or the differentiation capacities of multipotent NG2+ precursor cells, or both, to initiate glioma formation. We, indeed, have clearly shown that, *in vitro*, tumor cells are severely compromised in their terminal differentiation abilities (Figure 5 ). These results are in agreement with a recent study showing that immortalized neural progenitor cells derived from ENU-treated rats were unable to differentiate into neural lineages [31]. Finally, we have demonstrated that changes in cell-cell interactions and environment cues induced drastic immunophenotype modifications as well as an increase in cell proliferation of tumor cells derived from rat low grade glioma (Figure 5 and Supplemental Figure 3 ). This highlights that the homogenous character and non proliferative features identified in rat low grade glioma *in situ* are likely due to the tumor microenvironment.

In summary, taken together our results strongly suggest that multipotent NG2-expressing glial precursor cells are a new potential glioma cell initiating population in N-ethyl-N-nitrosourea- induced gliomagenesis. Another possible scenario is that an initial mutation has

occurred within a true stem cell early on and that mutation is only revealed in downstream precursor cells. In order to address the presence of stem-like cells in rat low grade glioma we subjected rat brains to radiations (Figure 6 ). We observed that some tumor cells were still present upon irradiation. These cells retained characteristics of NG2+ precursor cells and did not express the neural stem cell markers nestin and IQGAP1.

Moreover, in contrast to glioblastoma [5 ], we were not able to produce neurospheres from rat ENU-induced low grade glioma, pointing out the absence of typical cancer stem-like cells within these tumors. Given that tumor sizes are quite small and that tumoral NG2 + cells cannot be expanded *in vitro* , testing the tumorigenic potential of these cells is truly challenging. Since low grade glioma homogeneously express the NG2 marker and that cell-cell contacts and signals from environment seem to be crucial for survival of NG2+ tumor cells, another way to address the tumorigenicity of those cells might be to directly transplant tumor pieces into different brain regions of immunocompromised mouse strains. Overall this makes the cancer stem cell hypothesis as the origin of rat ENU-induced oligodendroglioma quite unlikely.

This study might also open up new perspectives for understanding several features of the human disease. Low grade rat gliomas showed histological characteristics that are similar to human oligodendroglioma. Those includes homogenous cellularity, uniform cells with minimal process formation, regular round nuclei, and arborizing capillary network that stained with collagen IV and IQGAP1 antibodies [5 ]. Rat tumor cells also express sets of genes (i.e NG2, PDGF $\alpha$ -R, Olig2, Sox10 and Nkx2.2) that are also preferentially found in human oligodendroglioma and oligoastrocytoma. [32 ,35 ,37 ]. The capability for rat oligodendroglioma-derived cells to express mosaic immunophenotypes when grown *in vitro* (Figure 5 ) could provide an explanation about the cell heterogeneity observed in high grade human oligodendroglioma which often makes their respective classification difficult or even impossible [7 ]. Rat glioma cells were able to express the neuronal marker  $\beta$ III-tubulin (Figure 5f ) which would explain why oligodendroglioma frequently display immunohistochemical and ultrastructural features of neuronal cells [46 ]. Moreover, we demonstrated that rat glioma cells exhibit aberrant co-expression of both astrocytic and oligodendroglial cell lineage markers (Figure 5e ), thus providing a rationale for similar genetic signatures identified in both astrocytic and oligodendrocytic components in mixed human oligoastrocytoma [47 ]. Although one has to be cautious before extrapolating rat models to human pathologies, similarities between rat low grade glioma and human oligodendroglioma might provide clues to explain some characteristics of the human disease and further understand how glioma emerge and develop over time in order to design new therapies aiming at curing brain tumors.

## Acknowledgements:

We thank Dr. H. Chneiweiss for Olig2 antibody, Dr. M. Wegner for SOX10 antibody, Dr. T. Buchou for stimulating discussion and N. Chaumontel for technical assistance. This work was supported by grants from the Association pour la Recherche sur le Cancer to JB (ARC N° 4725) and INCA to JB, JH, FE and CR (PL114).

## References:

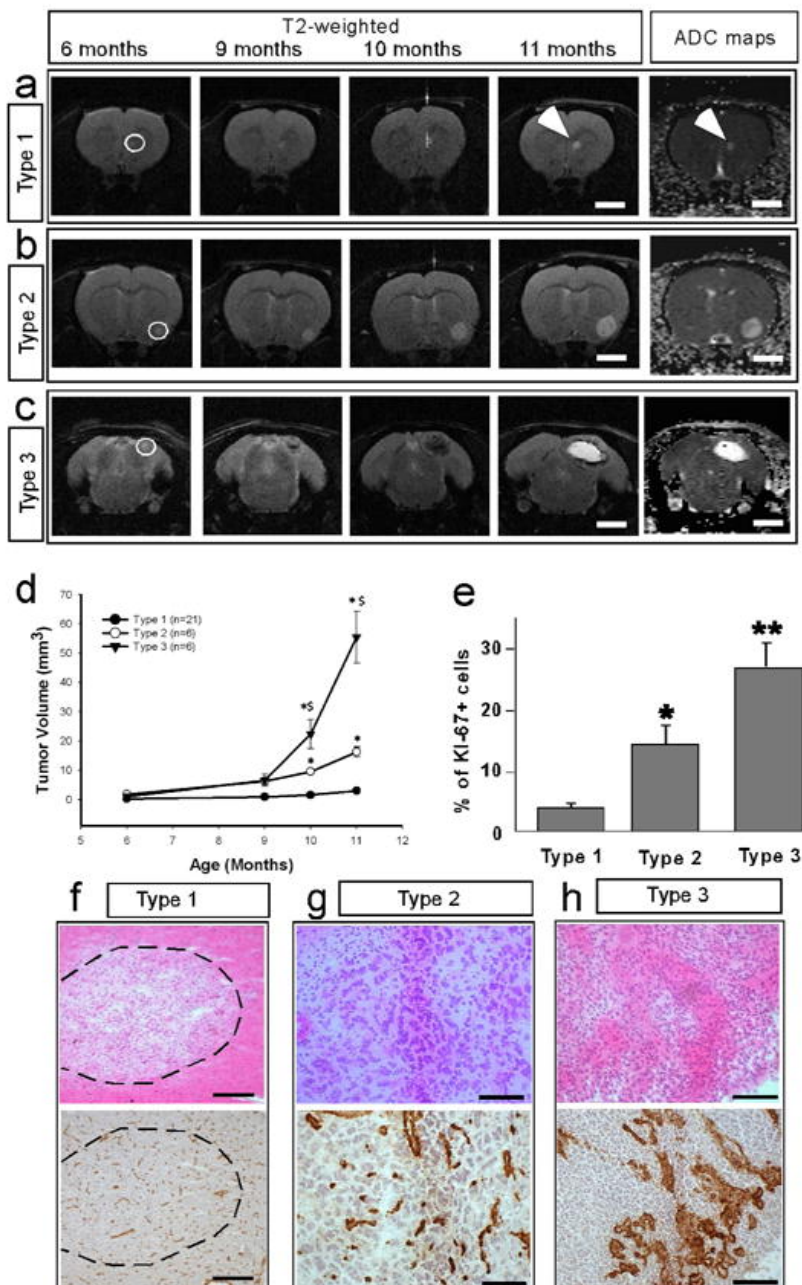
- 1 . Gilbertson RJ , Rich JN . 2007 ; Making a tumour's bed: glioblastoma stem cells and the vascular niche . *Nat Rev Cancer* . 7 : 733 - 6
- 2 . Hemmati HD , Nakano I , Lazareff JA , Masterman-Smith M , Geschwind DH , Bronner-Fraser M , Kornblum HI . 2003 ; Cancerous stem cells can arise from pediatric brain tumors . *Proc Natl Acad Sci U S A* . 100 : 15178 - 83
- 3 . Galli R , Binda E , Orfanelli U , Cipelletti B , Gritti A , De Vitis S , Fiocco R , Foroni C , Dimeco F , Vescovi A . 2004 ; Isolation and characterization of tumorigenic, stem-like neural precursors from human glioblastoma . *Cancer Res* . 64 : 7011 - 21
- 4 . Singh SK , Hawkins C , Clarke ID , Squire JA , Bayani J , Hide T , Henkelman RM , Cusimano MD , Dirks PB . 2004 ; Identification of human brain tumour initiating cells . *Nature* . 432 : 396 - 401
- 5 . Balenci L , Clarke ID , Dirks PB , Assard N , Ducray F , Jouvett A , Belin MF , Honnorat J , Baudier J . 2006 ; IQGAP1 protein specifies amplifying cancer cells in glioblastoma multiforme . *Cancer Res* . 66 : 9074 - 82
- 6 . Bao S , Wu Q , McLendon RE , Hao Y , Shi Q , Hjelmeland AB , Dewhirst MW , Bigner DD , Rich JN . 2006 ; Glioma stem cells promote radioresistance by preferential activation of the DNA damage response . *Nature* . 444 : 756 - 60
- 7 . Perry JR . 2001 ; Oligodendrogliomas: clinical and genetic correlations . *Curr Opin Neurol* . 14 : 705 - 10
- 8 . Mason WP . 2005 ; Oligodendroglioma . *Curr Treat Options Neurol* . 7 : 305 - 314
- 9 . Weiss WA , Burns MJ , Hackett C , Aldape K , Hill JR , Kuriyama H , Kuriyama N , Milshteyn N , Roberts T , Wendland MF , DePinho R , Israel MA . 2003 ; Genetic determinants of malignancy in a mouse model for oligodendroglioma . *Cancer Res* . 63 : 1589 - 95
- 10 . Uhrbom L , Dai C , Celestino JC , Rosenblum MK , Fuller GN , Holland EC . 2002 ; Ink4a-Arf loss cooperates with KRas activation in astrocytes and neural progenitors to generate glioblastomas of various morphologies depending on activated Akt . *Cancer Res* . 62 : 5551 - 8
- 11 . Ohgaki H , Kita D , Favreux A , Huang H , Homma T , Dessen P , Weiss WA , Kleihues P , Heppner FL . 2006 ; Brain tumors in S100beta-v-erbB transgenic rats . *J Neuropathol Exp Neurol* . 65 : 1111 - 7
- 12 . Ding H , Guha A . 2001 ; Mouse astrocytoma models: embryonic stem cell mediated transgenesis . *J Neurooncol* . 53 : 289 - 96
- 13 . Dai C , Celestino JC , Okada Y , Louis DN , Fuller GN , Holland EC . 2001 ; PDGF autocrine stimulation dedifferentiates cultured astrocytes and induces oligodendrogliomas and oligoastrocytomas from neural progenitors and astrocytes in vivo . *Genes Dev* . 15 : 1913 - 25
- 14 . Holland EC , Celestino J , Dai C , Schaefer L , Sawaya RE , Fuller GN . 2000 ; Combined activation of Ras and Akt in neural progenitors induces glioblastoma formation in mice . *Nat Genet* . 25 : 55 - 7
- 15 . Holland EC , Li Y , Celestino J , Dai C , Schaefer L , Sawaya RA , Fuller GN . 2000 ; Astrocytes give rise to oligodendrogliomas and astrocytomas after gene transfer of polyoma virus middle T antigen in vivo . *Am J Pathol* . 157 : 1031 - 7
- 16 . Lindberg N , Kastemar M , Olofsson T , Smits A , Uhrbom L . 2009 ; Oligodendrocyte progenitor cells can act as cell of origin for experimental glioma . *Oncogene* . 28 : 2266 - 75
- 17 . Uhrbom L , Hesselager G , Nister M , Westermarck B . 1998 ; Induction of brain tumors in mice using a recombinant platelet-derived growth factor B-chain retrovirus . *Cancer Res* . 58 : 5275 - 9

- 18 . Assanah M , Lochhead R , Ogden A , Bruce J , Goldman J , Canoll P . 2006 ; Glial progenitors in adult white matter are driven to form malignant gliomas by platelet-derived growth factor-expressing retroviruses . *J Neurosci* . 26 : 6781 - 90
- 19 . Kish PE , Blaivas M , Strawderman M , Muraszko KM , Ross DA , Ross BD , McMahon G . 2001 ; Magnetic resonance imaging of ethyl-nitrosourea- induced rat gliomas: a model for experimental therapeutics of low-grade gliomas . *J Neurooncol* . 53 : 243 - 57
- 20 . Koestner A . 1990 ; Characterization of N-nitrosourea-induced tumors of the nervous system; their prospective value for studies of neurocarcinogenesis and brain tumor therapy . *Toxicol Pathol* . 18 : 186 - 92
- 21 . Vaquero J , Coca S , Moreno M , Oya S , Arias A , Zurita M , Morales C . 1992 ; Expression of neuronal and glial markers in so-called oligodendroglial tumors induced by transplacental administration of ethyl-nitrosourea in the rat . *Histol Histopathol* . 7 : 647 - 51
- 22 . Zook BC , Simmens SJ , Jones RV . 2000 ; Evaluation of ENU-induced gliomas in rats: nomenclature, immunochemistry, and malignancy . *Toxicol Pathol* . 28 : 193 - 201
- 23 . Bilzer T , Reifenberger G , Wechsler W . 1989 ; Chemical induction of brain tumors in rats by nitrosoureas: molecular biology and neuropathology . *Neurotoxicol Teratol* . 11 : 551 - 6
- 24 . Slikker W 3rd , Mei N , Chen T . 2004 ; N-ethyl-N-nitrosourea (ENU) increased brain mutations in prenatal and neonatal mice but not in the adults . *Toxicol Sci* . 81 : 112 - 20
- 25 . Dawson MR , Polito A , Levine JM , Reynolds R . 2003 ; NG2-expressing glial progenitor cells: an abundant and widespread population of cycling cells in the adult rat CNS . *Mol Cell Neurosci* . 24 : 476 - 88
- 26 . Bouslama-Oueghlani L , Wehrle R , Sotelo C , Dusart I . 2005 ; Heterogeneity of NG2-expressing cells in the newborn mouse cerebellum . *Dev Biol* . 285 : 409 - 21
- 27 . Belachew S , Chittajallu R , Aguirre AA , Yuan X , Kirby M , Anderson S , Gallo V . 2003 ; Postnatal NG2 proteoglycan-expressing progenitor cells are intrinsically multipotent and generate functional neurons . *J Cell Biol* . 161 : 169 - 86
- 28 . Aguirre A , Gallo V . 2004 ; Postnatal neurogenesis and gliogenesis in the olfactory bulb from NG2-expressing progenitors of the subventricular zone . *J Neurosci* . 24 : 10530 - 41
- 29 . Aguirre AA , Chittajallu R , Belachew S , Gallo V . 2004 ; NG2-expressing cells in the subventricular zone are type C-like cells and contribute to interneuron generation in the postnatal hippocampus . *J Cell Biol* . 165 : 575 - 89
- 30 . Balenci L , Saoudi Y , Grunwald D , Deloulme JC , Bouron A , Bernards A , Baudier J . 2007 ; IQGAP1 regulates adult neural progenitors in vivo and vascular endothelial growth factor-triggered neural progenitor migration in vitro . *J Neurosci* . 27 : 4716 - 24
- 31 . Savarese TM , Jang T , Low HP , Salmonsens R , Litofsky NS , Matuasevic Z , Ross AH , Recht LD . 2005 ; Isolation of immortalized, INK4a/ARF-deficient cells from the subventricular zone after in utero N-ethyl-N-nitrosourea exposure . *J Neurosurg* . 102 : 98 - 108
- 32 . Shoshan Y , Nishiyama A , Chang A , Mork S , Barnett GH , Cowell JK , Trapp BD , Staugaitis SM . 1999 ; Expression of oligodendrocyte progenitor cell antigens by gliomas: implications for the histogenesis of brain tumors . *Proc Natl Acad Sci U S A* . 96 : 10361 - 6
- 33 . Rivers LE , Young KM , Rizzi M , Jamen F , Psachoulia K , Wade A , Kessaris N , Richardson WD . 2008 ; PDGFRA/NG2 glia generate myelinating oligodendrocytes and piriform projection neurons in adult mice . *Nat Neurosci* . 11 : 1392 - 401
- 34 . Wegner M . 2008 ; A matter of identity: transcriptional control in oligodendrocytes . *J Mol Neurosci* . 35 : 3 - 12
- 35 . Riemenschneider MJ , Koy TH , Reifenberger G . 2004 ; Expression of oligodendrocyte lineage genes in oligodendroglial and astrocytic gliomas . *Acta Neuropathol* . 107 : 277 - 82
- 36 . Rhee W , Ray S , Yokoo H , Hoane ME , Lee CC , Mikheev AM , Horner PJ , Rostomily RC . 2009 ; Quantitative analysis of mitotic Olig2 cells in adult human brain and gliomas: implications for glioma histogenesis and biology . *Glia* . 57 : 510 - 23
- 37 . Bannykh SI , Stolt CC , Kim J , Perry A , Wegner M . 2006 ; Oligodendroglial-specific transcriptional factor SOX10 is ubiquitously expressed in human gliomas . *J Neurooncol* . 76 : 115 - 27
- 38 . Kondo T , Raff M . 2000 ; Oligodendrocyte precursor cells reprogrammed to become multipotential CNS stem cells . *Science* . 289 : 1754 - 7
- 39 . Tang DG , Tokumoto YM , Apperly JA , Lloyd AC , Raff MC . 2001 ; Lack of replicative senescence in cultured rat oligodendrocyte precursor cells . *Science* . 291 : 868 - 71
- 40 . Lwin Z , Gan HK , Mason WP . 2009 ; Low-grade oligodendroglioma: current treatments and future hopes . *Expert Rev Anticancer Ther* . 9 : 1651 - 61
- 41 . Deloulme JC , Raponi E , Gentil BJ , Bertacchi N , Marks A , Labourdette G , Baudier J . 2004 ; Nuclear expression of S100B in oligodendrocyte progenitor cells correlates with differentiation toward the oligodendroglial lineage and modulates oligodendrocytes maturation . *Mol Cell Neurosci* . 27 : 453 - 65
- 42 . Levison SW , Young GM , Goldman JE . 1999 ; Cycling cells in the adult rat neocortex preferentially generate oligodendroglia . *J Neurosci Res* . 57 : 435 - 46
- 43 . Dawson MR , Levine JM , Reynolds R . 2000 ; NG2-expressing cells in the central nervous system: are they oligodendroglial progenitors? . *J Neurosci Res* . 61 : 471 - 9
- 44 . Mallon BS , Shick HE , Kidd GJ , Macklin WB . 2002 ; Proteolipid promoter activity distinguishes two populations of NG2-positive cells throughout neonatal cortical development . *J Neurosci* . 22 : 876 - 85
- 45 . Nunes MC , Roy NS , Keyoung HM , Goodman RR , McKhann G 2nd , Jiang L , Kang J , Nedergaard M , Goldman SA . 2003 ; Identification and isolation of multipotential neural progenitor cells from the subcortical white matter of the adult human brain . *Nat Med* . 9 : 439 - 47
- 46 . Vyberg M , Ulhoi BP , Teglbjaerg PS . 2007 ; Neuronal features of oligodendrogliomas--an ultrastructural and immunohistochemical study . *Histopathology* . 50 : 887 - 96
- 47 . Kraus JA , Koopmann J , Kaskel P , Maintz D , Brandner S , Schramm J , Louis DN , Wiestler OD , von Deimling A . 1995 ; Shared allelic losses on chromosomes 1p and 19q suggest a common origin of oligodendroglioma and oligoastrocytoma . *J Neuropathol Exp Neurol* . 54 : 91 - 5

**Figure 1**

Visualization and development of rat ENU-induced glioma

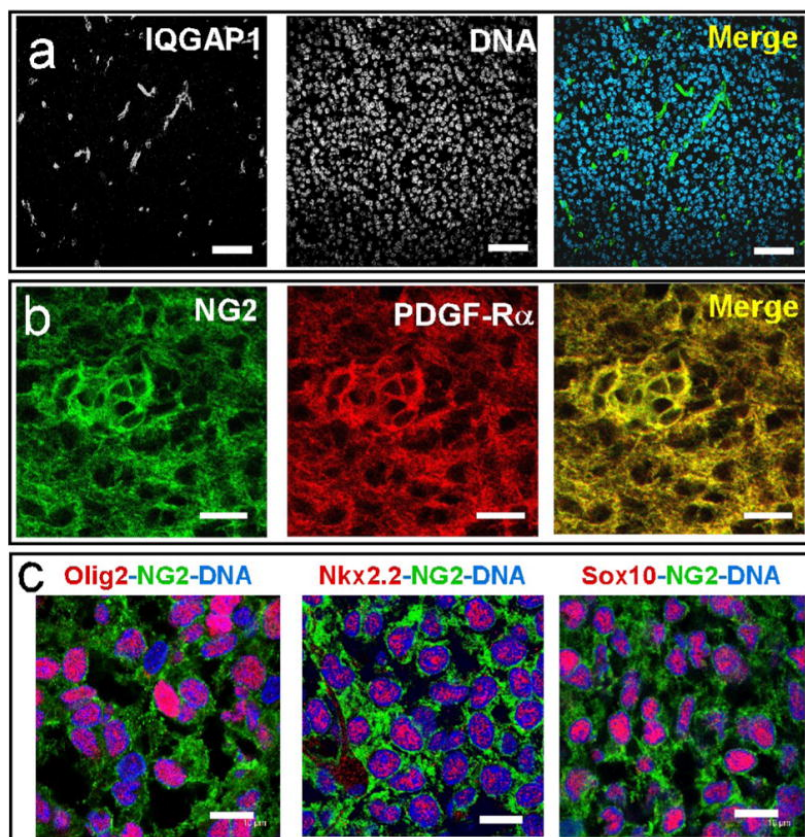
a–c: Typical T2-weighted MR images of the follow-up of 3 different types of ENU-induced tumors up to 11 months along the apparent diffusion coefficient (ADC) measured at 11 months. ENU-induced tumors are classified as Type 1 (a), Type 2 (b) and Type 3 (c) glioma according to their location and evolution. Initial lesions are circled in white. In panel a, arrow heads point to a typical low-grade type 1 glioma. Bar= 4mm. d: Different volume quantifications from MRI scans allowed us to distinguish 3 typical growth profiles over a period of 11 months (n=21 for type 1, n=6 for type 2 and n=6 for type 3). Type 3 glioma accounts for the most aggressive and malignant brain tumors. Error bars represent SEM. \*,  $p < 0.05$  vs type 1, \$,  $p < 0.01$  vs Type 2 (Two-Way Anova) e: Quantification of proliferating rate in Type 1, 2 and 3 induced glioma in 11-month-old rats. Tumor slices were stained with Ki-67 antibodies and counterstained with Hoechst marker. Student's t-test was applied, \* P-Value  $< 0.05$  and \*\* P-Value  $< 0.01$  compared to Type 1 glioma. f–h: Histological analysis of rat ENU-induced Type 1 (f), Type 2 (g), and Type 3 (h) glioma stained with hematoxylin and eosin (upper panels) and immunostained with collagen IV to visualize blood vessels (lower panels). In f, the dashed line circles the tumor bulk. Bars=200 $\mu$ m (a); Bar=100 $\mu$ m (b and c).



**Figure 2**

Immunohistochemical characterization of rat low-grade glioma

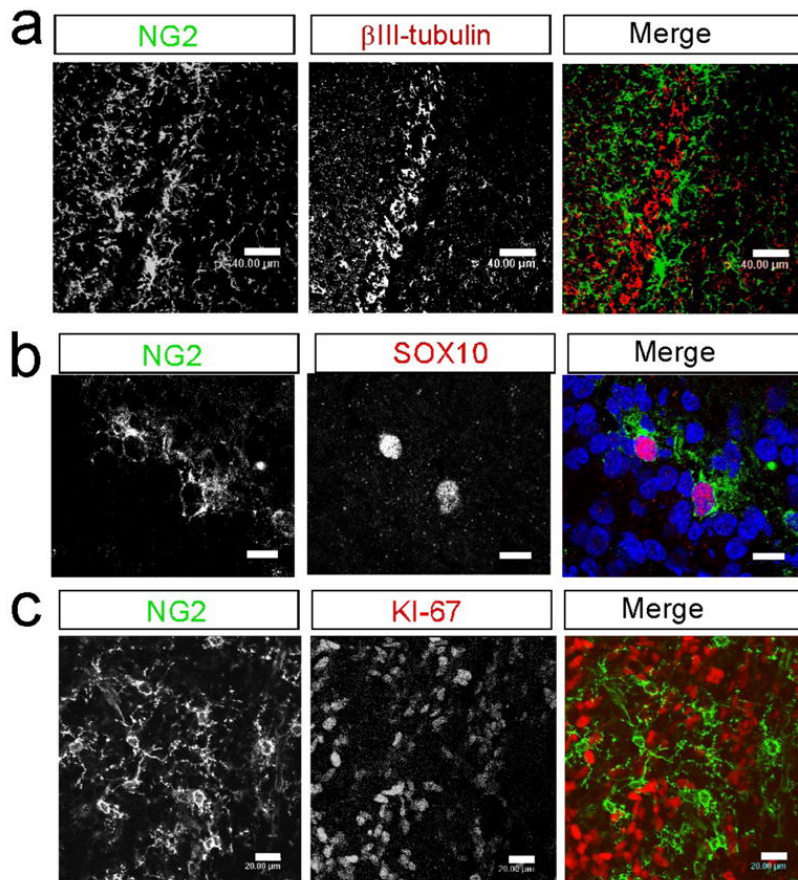
a: Microscope analysis of a low-grade tumor of a 9-month-old rat stained with IQGAP1 antibodies and counterstained with Hoechst (DNA). IQGAP1 is only present in blood vessels. Bar= 50  $\mu$ m. b: Confocal microscope analysis of a low-grade tumor of a 9-month-old rat co-immunostained with NG2 (green) and PDGF $\alpha$ -R (red) antibodies. Merge image demonstrate a colocalization of NG2 and PDGF $\alpha$ -R markers. Bar= 20 $\mu$ m. c: Confocal microscope analysis of a low-grade tumor of a 9-month-old rat co-immunostained for the nuclear markers Olig2, Nkx2.2 and Sox10 as indicated (red), NG2 (green) and Hoechst (DNA, blue). Bar=10 $\mu$ m.



**Figure 3**

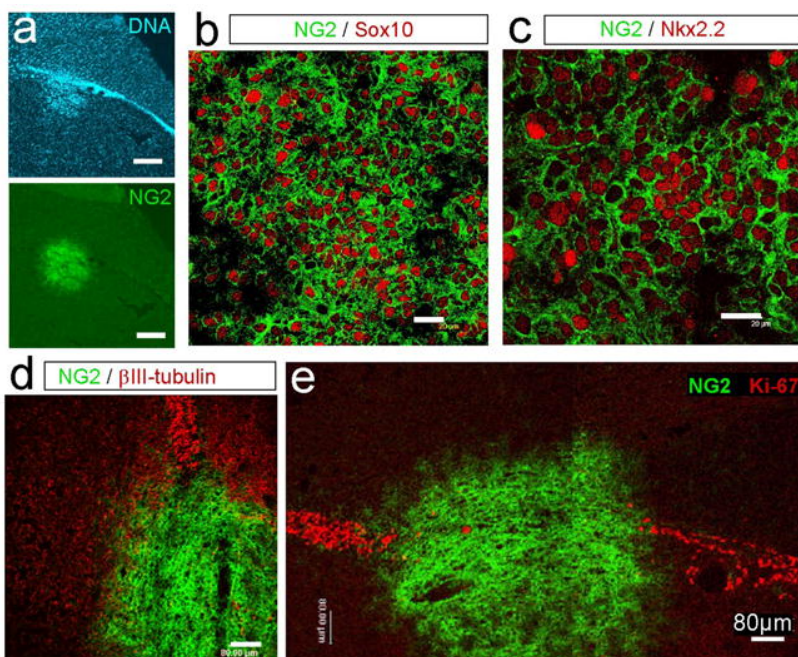
Identification of slow dividing NG2+ precursor cells in the rostral migratory stream of 3 month-old rats

a-c: Confocal analysis of coronal rat brain sections in the proximal (a and b) and the most distal part (c) of the RMS area double stained for NG2 (green) and  $\beta$ III-tubulin (red) (a; Bar= 40 $\mu$ m); triple stained for NG2 (green) Sox10 (red) and DNA (blue) (b; Bar= 10 $\mu$ m); or double stained for NG2 (green) and Ki-67 (red) (c; Bar= 20 $\mu$ m).

**Figure 4**

Characterization of slow dividing NG2+ glioma cells in early hyperplastic lesions in the rostral migratory stream

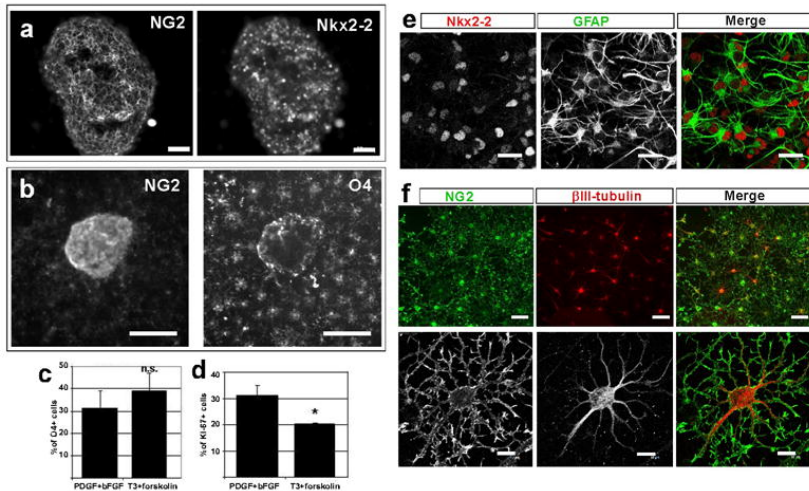
a: Brain sections of 3-month old rats stained with NG2 antibodies and counterstained with Hoechst (DNA) to visualize emerging ENU-induced tumors in the RMS, Bar=200 $\mu$ m. b-c: Confocal analysis of low-grade glioma located within the RMS and double stained for NG2 (green) and Sox 10 (red) (b; Bar=20 $\mu$ m), NG2 (green) and Nkx2.2 (red) (c; Bar=20 $\mu$ m), d-e: Confocal analysis of a low-grade glioma located within the RMS and double stained for NG2 (green) and  $\beta$ III-tubulin (red) or for NG2 (green) and Ki-67 (red) (d-e; Bar=80 $\mu$ m).



**Figure 5**

Immunocytochemical characteristics of rat low-grade glioma-derived explants

a: Tumor-derived explants in proliferating conditions in presence of both PDGF and bFGF were double immunostained with NG2 and Nkx2.2 antibodies. Bar=50µm. b: Microscope observation of a glioma-derived explant grown 6 days in culture medium supplemented with PDGF and bFGF and double immunostained with NG2 (green) and O4 (red) antibodies. Bar=200µm c: Quantification of O4+ cells of 6 day-explant cultures in proliferating (PDGF + bFGF) and differentiating (T3 + forskolin) conditions. d: Quantification of Ki-67+ cells of 6 day-explant cultures in proliferation and differentiation media. Results show a small decrease of proliferation in differentiating conditions. \* Student's T-Test, P-Value<0.05. e-f: Tumor cells migrating away from glioma explants in culture medium supplemented with PDGF and bFGF were double immunostained with Nkx2.2 (red) and GFAP (red) antibodies (e), or double immunostained with NG2 (green) and  $\beta$ III-tubulin (red) antibodies (f). Bar=20µm in e. Bar=50µm in f upper panels and Bar=10µm in f lower panels.

**Figure 6**

Response of low-grade glioma to radiations

a: MRI follow-up of a 0,8 mm<sup>3</sup> low-grade glioma located in the corpus callosum of a 6 month-old rat, before (- 4 days) and after irradiation from 4 to 137 days. At day 0, rats were irradiated with a single dose of 15 Gy. b: Regression curve of the low-grade tumor shown in panel a. By 10 days, the tumor size decreases by about 25% to reach 0,060 mm<sup>3</sup> at day 137. c: Hematoxylin and eosin stainings revealed a residue of tumorigenic tissue in the corpus callosum at day 137 post irradiation. Bar=200µm. d: Radio-resistant tumor cells strongly expressed Olig2 and Sox10 but did not express neither nestin nor IQGAP1. Bar=10 µm except for the left panel, Olig2 staining, bar=40µm.

